Original Article

OPEN

Developmental conditioning of endothelium-derived hyperpolarizing factor-mediated vasorelaxation

Rebecca Stead[a,*], Moji G. Musa[a,*], Claire L. Bryant[a], Stuart A. Lanham[b], David A. Johnston[c], Richard Reynolds[a], Christopher Torrens[a], Paul A. Fraser[d], and Geraldine F. Clough[a]

Objectives: The endothelium maintains vascular homeostasis through the release of endothelium-derived relaxing factors (EDRF) and endothelium-derived hyperpolarization (EDH). The balance in EDH : EDRF is disturbed in cardiovascular disease and may also be susceptible to developmental conditioning through exposure to an adverse uterine environment to predispose to later risk of hypertension and vascular disease.

Methods: Developmentally conditioned changes in EDH : EDRF signalling pathways were investigated in cremaster arterioles (18–32 μm diameter) and third-order mesenteric arteries of adult male mice offspring of dams fed either a fat-rich (high fat, HF, 45% energy from fat) or control (C, 10% energy from fat) diet. After weaning, offspring either continued on high fat or were placed on control diets to give four dietary groups (C/C, HF/C, C/HF, and HF/HF) and studied at 15 weeks of age.

Results: EDH via intermediate (IK_{Ca}) and small (SK_{ca}) conductance calcium-activated potassium channels contributed less than 10% to arteriolar acetylcholine-induced relaxation in in-situ conditioned HF/C offspring compared with $\sim$60% in C/C ($P < 0.01$). The conditioned reduction in EDH signalling in HF/C offspring was reversed in offspring exposed to a high-fat diet both before and after weaning (HF/HF, 55%, $P < 0.01$ vs. HF/C). EDH signalling was unaffected in arterioles from C/HF offspring. The changes in EDH : EDRF were associated with altered endothelial cell expression and localization of IK_{Ca} channels.

Conclusion: This is the first evidence that EDH-mediated microvascular relaxation is susceptible to an adverse developmental environment through down-regulation of the IK_{Ca} signalling pathway. Conditioned offspring exposed to a 'second hit' (HF/HF) exhibit adaptive vascular mechanisms to preserve dilator function.

Keywords: developmental conditioning, endothelium derived hyperpolarizing factor, intermediate conductance calcium-activated potassium channels, maternal obesity, microvasculature

Abbreviations: ACh, acetylcholine; DAPI, 4,6-diamidino-2-phenylindole; EDHF, endothelium-derived hyperpolarizing factor; EDRF, endothelium-derived relaxing factor; eNOS, endothelial nitric oxide synthase; IEL, internal elastic lamina; IK_{Ca}, intermediate-conductance calcium-activated potassium channel; L-NAME, N$^{\omega}$-nitro-L-arginine methyl ester hydrochloride; PBST, PBS 0.1% Tween-20; ROI, region of interest; SK_{Ca}, small-conductance calcium-activated potassium channel; TRAM-34, 1-[(2-chlorophenyl)diphenylmethyl]-1H-pyrazole

INTRODUCTION

The endothelium maintains vascular homeostasis through the release of endothelium-derived relaxing factors (EDRF; including nitric oxide, prostaglandins [PGE_2, PGI_2]), and endothelium-derived hyperpolarization (EDH). Ageing and pathologies, including hypertension, obesity, and type 2 diabetes mellitus are associated with a reduced nitric oxide-dependent vasodilator capacity in the resistance vasculature [1–5]. It remains contentious whether EDH signalling is similarly affected in cardio-metabolic disease [6]. Persistence or even upregulation of EDH-mediated relaxation to compensate for the loss of nitric oxide-mediated relaxation has been reported in small resistance arteries and arterioles from animal models of hypertension [7], diet-induced obesity [8,9], and hypercholesterolaemia [10,11] whereas in other models reduced EDH-dilator responses are reported [12,13]. Similarly, conflicting findings of the degree of dysfunction of EDH-mediated relaxation have been reported in humans with essential hypertension, atherosclerosis, and diabetes [6].

It is now widely accepted that an adverse early life environment primes or conditions multiple systems and pathways to increase susceptibility in the offspring to later disease risk [14,15]. Evidence from both animal studies and human cohorts indicates that offspring exposed to a

disadvantageous developmental environment go on to develop endothelial dysfunction in later life [16] and that maternal under and over-nutrition condition both EDRF and EDH-mediated vasorelaxation [11,17–19]. These studies were conducted in resistance and large conduit arteries in which nitric oxide-mediated signalling predominates. Direct evidence of the impact of the developmental environment on endothelium-mediated relaxation within arterioles in the microvasculature (vessels <200 μm in diameter) where EDH-mediated relaxation play a greater role is missing [20].

Intermediate (IK_{Ca} 3.1) and small (SK_{Ca} 2.3) conductance calcium-activated potassium channels play a prominent role in initiating hyperpolarization and modulating electrical conduction along the endothelium and to the smooth muscle of small arteries and arterioles in many vascular beds [6,21,22]. These channels may also contribute to the modulation of endothelial Ca^{2+} signalling and nitric oxide release [23]. Obesity-related disorders are associated with impairment in the signalling mechanisms of both IK_{Ca} and SK_{Ca} channels [12]. Deficiencies in IK_{Ca} and SK_{Ca} channels have also been reported in diabetes [13] and ageing [24], and genetic deficits in IK_{Ca} and SK_{Ca} shown to lead to elevated arterial blood pressure (BP) in mice [25]. Conversely, increased function and expression of IK_{Ca} and SK_{Ca} channels may contribute to sustained endothelium-dependent relaxation in the early stages of obesity [9]. IK_{Ca} and SK_{Ca} channel expression and location have been shown to be subject to significant remodelling during development [26] and ageing [24]. However, the mechanisms underlying altered membrane expression and/or activity of K_{Ca} channels have yet to be determined [27].

The present study was designed to test the impact of developmental conditioning through exposure to fat-rich diet during gestation and suckling on the contribution of the EDH-signalling to vasodilatation within a skeletal muscle microvascular bed. It also set out to determine whether dysregulation of K_{Ca} channel signalling plays a mechanistic role. As we have previously shown that a second insult (a postweaning fat-rich diet) independently influences vascular outcomes and interacts with the effects of an adverse intra-uterine environment [28], we now examine whether the EDH-signalling pathway in developmentally conditioned adult mouse offspring is exacerbated in conditioned offspring additionally fed a HF-rich postweaning.

METHODS

Ethical approval
All animal experimentation was performed under license from the Home Office in accordance with the Animals (Scientific Procedures) Act (1986). The study received institutional approval from the University of Southampton Biomedical Research Facility Research Ethics Committee.

Animal procedures
All mice were reared within the University of Southampton Biomedical Research Facility and were housed in appropriate environments in rooms maintained at $22 \pm 2°C$ with a 12 h light : dark cycle. Female C57/BL6 mice were fed either a fat-rich (HF, standardized Van Heek diet-induced obesity diet) [29] with 45% energy from fat, 35% from carbohydrate and 18% from protein (TestDiet, St. Louis, Missouri, USA, $n = 21$) or control diet with 10% energy from fat, 72% from carbohydrate and 18% from protein (RM1 chow diet, Special Diets Services, Witham, UK, $n = 17$) for 4 weeks before conception and throughout gestation and lactation as previously described [28,30]. Dams' body weight and body composition were measured after weaning of their offspring. Litter sizes were standardized at birth and female offspring culled at weaning (21 days). After weaning, male offspring were fed either the same diet as their dams or diet switched to give four offspring groups (C/C, C/HF, HF/C, and HF/HF). Offspring BP was measured via tail cuff plethysmography (Columbus Volumetric BP Monitor NIBP-8, Linton Instruments, Diss, UK) at 15 weeks of age. After overnight fasting, animals were killed by cervical dislocation and body weight and body composition measured. Blood was collected by cardiac puncture following euthanasia for measurement of fasting plasma glucose (Accu-Check; Roche, Mannheim, Germany) and total plasma lipids by gas chromatography [31].

Measurement of body composition using three-dimensional computed tomography
Whole animal carcasses were scanned using a Skyscan 1176 in-vivo micro-computed tomography (CT) scanner (Bruker microCT, Kontich, Belgium). All scans were taken at 40 kV, 600 μA with 0.2 mm aluminium filter, with 0.7° rotation step. Individual two-dimensional cross-sectional images were reconstructed using Bruker NRecon software version 1.6.5.8. Voxel resolution was 35 μm. Reconstructed images were analysed using Bruker CTAn software version 1.13.5.1 with appropriate thresholds to determine volumes of fat, soft tissue, and bone [32].

Cremaster arteriolar function
Immediately after killing by cervical dislocation, the abdominal aorta was cannulated orthogradely and the circulation stabilized by perfusion with a cardioplegic solution that contained NaCl (110 mmol/l), $MgCl_2$ (16 mmol/l), KCl (16 mmol/l), $CaCl_2$ (1.2 mmol/l), $NaHCO_3$ (10 mmol/l), isoprenaline hydrochloride (0.01 mmol/l; to ensure full vasodilatation), ascorbic acid (0.01 mmol/l; to prevent the oxidation of isoprenaline) and heparin (300 IU/ml). The pH was adjusted to 7.0 ± 0.05. All chemicals were purchased from Sigma-Aldrich (Dorset, UK). The cremaster muscle was exteriorized as described previously [33] and perfusion switched to Krebs solution (NaCl (118 mmol/l); KCl (4.7 mmol/l); $CaCl_2$ (2.52 mmol/l); $MgSO_4.7H_2O$ (1.18 mmol/l); KH_2PO_4 (1.18 mmol/l), $NaHCO_3$ (25 mmol/l), glucose (9 mmol/l) buffered to pH 7.4 ± 0.05) containing bovine serum albumin (10 mg/ml) at a rate of 0.5 ml/min. The exteriorized cremaster was continuously superfused with a similar but albumin-free Krebs solution (pH 7.4) gassed with 5% CO_2 in air and maintained at 37°C at a rate of 2 ml/min. After a stabilization period of 30 min a bolus of fluorescein isothiocyanate conjugated-albumin (10 mg/ml) in Krebs solution was injected into the circulation via the abdominal aorta and suitable 3A cremaster arterioles (<40 μm diameter) identified. The cremaster muscle was trans-illuminated using blue (480–500 nm) light and viewed
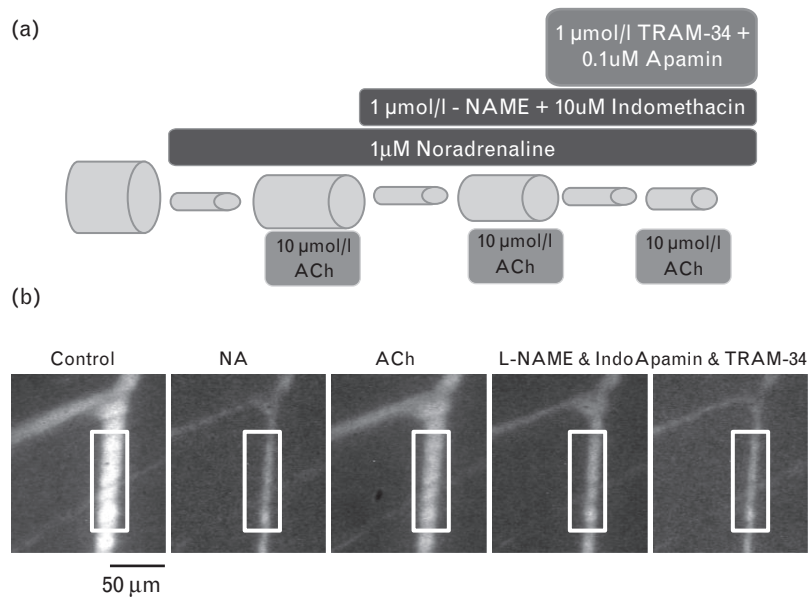
(a)

(b)

FIGURE 1 Functional studies. (a) Diagrammatic representation of protocol for measurement of functional relaxation in the cremaster microvasculature. (b) The average diameter of a vessel segment was estimated from the fraction of the pixels within the region of interest (shown by the white box) above a predetermined threshold level. The threshold was calculated from the time series of images obtained during the different treatments by using the 'Stack Histogram' function using the 'Yen' algorithm in Image J (1.49 v) Auto Threshold v1.5. The diameter at any time point is given by the product of the width of the region of interest and f. NA, noradrenaline; ACh, acetyl choline; N^{ω}-nitro-L-arginine methyl ester hydrochloride; TRAM-34, 1-[(2-chlorophenyl) diphenylmethyl]-1H-pyrazole.

with a Zeiss ACM microscope using a 10× water immersion objective lens at an emission wavelength of 525–535 nm. Images of single arterioles were captured at $2\,s^{-1}$ via a ProGres MF cool camera (Jenoptik, Jena Germany) (Fig. 1).

To assess functional responses, vessels were preconstricted with 1 μmol/l noradrenaline followed by relaxation to 10 μmol/l acetylcholine (ACh) added as a bolus to the superfusate. Specific blockers to nitric oxide (100 μmol/l L-NAME), prostaglandins (10 μmol/l indomethacin) and IK_{Ca} (1-[(2-chlorophenyl)diphenylmethyl]-1H-pyrazole (TRAM-34) 1 μmol/l) and SK_{Ca} (apamin, 0.1 μmol/l) were then sequentially added to the superfusate to reveal the relative contribution of these pathways to ACh-endothelial-mediated relaxation (Fig. 1). Arteriolar diameters were measured off-line using Image Hopper (Samsara Research, Dorking, UK) and relaxation responses were represented as the maximum % reversal of noradrenaline-induced constriction. The reduction in relaxation at each stage of signalling pathway blockade was calculated as a fraction of the initial ACh-induced relaxation in the absence of blockers. Using these data, the relative fractional contribution of the EDRF-pathways (blockable by N^{ω}-nitro-L-arginine methyl ester hydrochloride (L-NAME) and indomethacin) and of EDH-mediated signalling (via IK_{Ca} and SK_{Ca} channels) to ACh-mediated relaxation was estimated in each offspring group.

Quantification of endothelial expression of intermediate-conductance calcium-activated potassium channel and small-conductance calcium-activated potassium channel in third-order cremaster arterioles and mesenteric arteries

The entire cremaster muscle was dissected in physiological saline solution (PSS, mmol/l: 119 NaCl, 4.7 KCl, 1.17 $MgSO_4$, 1.18 KH_2PO_4, 25 $NaHCO_3$, 0.027 EDTA, 5.5 glucose) and fixed in 4% paraformaldehyde overnight at 4°C. Areas of the cremaster muscle (~1 mm²) were then cut from either side of the main cremaster artery and blocked in 5% (v/v) goat serum, 1% BSA (v/v) 0.3 mol/l glycine, 2% Triton X-100 in 1x PBS (Sigma Aldrich) for 1 h. The cremaster samples were incubated with an IK_{Ca} antibody (APC-051 Alomone Labs, Jerusalem, Israel; 1 : 200) and CD31 antibody (Abcam, Cambridge UK; 1 : 100) overnight at 4°C. The tissues were washed three times with 1 × PBS 0.1% Tween-20 (PBST) followed by incubation with Image-iT FX signal enhancer (Invitrogen, Paisley, UK) for 30 min and then washed three times in PBST. Samples were probed with Alexa Fluor goat antimouse IgM 568 secondary antibody (Invitrogen; 1 : 100) and Alexa Fluor goat antirabbit IgG 633 secondary antibody (Invitrogen; 1 : 100) for 1 h followed by three washes in PBST and incubation with 4,6-diamidino-2-phenylindole (DAPI) for 30 min. Samples were cleared in 2,2'-thiodiethanol in stages; 10, 25, 50, 97% (in H_2O) each for 45 min with two incubations in 97% and mounted onto coverslips in 100% 2,2'-thiodiethanol.

Third-order fat free mesenteric arterioles (diameter 150−200 μm) were dissected into PBS and fixed as described above. The vessels were cut into 0.2 mm rings and opened longitudinally. Sections were mounted with the endothelium uppermost and blocked in 5% (v/v) goat serum, 1% BSA (v/v) 0.3 mol/l glycine, 0.2% Triton X-100 in 1 × PBS for 1 h followed by incubation with the IK_{Ca} antibody (APC-051 Alomone Labs; 1 : 100) or SK_{Ca} antibody (APC-025 Alomone; 1 : 50) for 2 h. Samples were washed three times in PBST then probed with Alexa Fluor 568 goat antimouse IgM secondary antibody followed by a further three washes in PBST. Sections were then incubated with Alexa Fluor 633 hydrazide (Invitrogen; 1 : 5000) for 30 min

and DAPI (1 : 1000) for 20 min before mounting in Mowiol. Negatives for all tissues and secondary antibodies were generated.

Tissues were imaged using a Leica TCS SP5 multiphoton confocal microscope and images analysed using Leica AS AF suite. Three regions of interest (ROIs, $45 \times 15\,\mu m$ for cremaster vessels and $40 \times 40\,\mu m$ for mesenteric arteries) per sample were examined. ROIs were selected based on clear vessel morphology, that is, away from branch points and avoiding areas of tissue where there was overlap of vessels through the cremaster. In the mesenteric artery, ROIs were chosen in areas of well preserved endothelial morphology and internal elastic lamina (IEL) structural integrity. The analysis of K_{Ca} channel expression (intensity) and location (overlap) was undertaken on maximum projection images from z-stacks of the whole vessel in cremaster and in the endothelial layer of mesenteric arteries excluding the smooth muscle cell layer. Overlap with endothelial cell membrane was semiquantified using Mander's overlap coefficient analysis [34]. Overlap was also explored in the cremaster arterioles using a single transverse median optical section of each vessel. Myoendothelial domains (number and size of holes in the IEL and colocalization of IK_{Ca} and SK_{Ca} were quantified in mesenteric segments.

eNOS mRNA expression in cremaster muscle

Freshly dissected cremaster muscles were powdered under liquid nitrogen and 75 mg of tissue homogenized in 1 ml Tri Reagent (Invitrogen) prior to centrifugation ($12\,000 \times g$ 10 min at 4°C). The supernatant was incubated with 1-bromo-3-chloropropane ($100\,\mu l$) for 15 min before centrifugation ($12\,000 \times g$ for 15 min 4°C) and transfer of the aqueous phase to a fresh microfuge tube. The samples were mixed with $500\,\mu l$ isopropanol (15 min) and recentrifuged at $12\,000 \times g$ for 15 min 4°C. The supernatant was removed and the pellet resuspended in 1 ml 75% ethanol and centrifuged $7500 \times g$ for 5 min. The pellet was resuspended in nuclease free H_2O and RNA concentration and quality (260/280 ratio) assessed using Nanodrop (Thermo Scientific, Basingstoke, UK) and stored at -80°C. cDNA was prepared as follows using Promega reagents. $1.3\,\mu g$ cremaster RNA was mixed with $1\,\mu l$ Oligo(dT) and $1\,\mu l$ random primer, the reactions were heated to 70°C for 5 min followed by addition of $5\,\mu l$ $5 \times$ reaction buffer, $1\,\mu l$ 10 mmol/l dNTPs, $0.5\,\mu l$ RNasin, $1\,\mu l$ reverse transcriptase Moloney murine leukemia virus reverse transcriptase and made to $25\,\mu l$ with nuclease free H_2O. The reactions were then incubated at 42°C for 60 min and then 70°C 15 min and the cDNA stored at -20°C prior to use in real time polymerase chain reaction (RT-PCR) RT-PCR. For each sample a triplicate reaction was made containing $5\,\mu l$ cDNA, $4\,\mu l$ nuclease free H_2O, $1\,\mu l$ $6\,\mu mol/l$ forward/reverse primer mix (eNOS: forward – GGAAATGTCAGGCCCGTACA reverse – GTCGAGCAG-GAGACACTGTTGA, GAPDH (PrimerDesign)) and $10\,\mu l$ $2\times$ Precision SYBR green master mix (PrimerDesign). Total 96 well plates were cycled at 95°C 10 min, followed by 40 cycles of 95°C 15 sec and 60°C 1 min followed by a melt curve stage in the Applied Biosystems StepOne Plus RT-PCR machine. The average deltaCT value of the mRNA of interest was normalized to glyceraldehyde-3-phosphate dehydrogenase (GAPDH) and a delta CT value generated by expressing results as fold increase compared with C/C.

Statistical analysis

No more than two offspring per dam were studied in any dietary group and where a variable was measured in two offspring from the same litter the values were treated as replicates and averaged. In functional studies no more than two arterioles were studied in any cremaster preparation and the values were treated as replicates and averaged. Data were tested for normality using the Shapiro–Wilks test. Data from dams were compared by unpaired Students t-test. In offspring groups, pre and postnatal dietary exposures were compared by two-way ANOVA followed by Bonferroni post hoc test using PASW version 21 (SPSS UK, Woking, UK). All data are expressed as mean $\pm$ SEM. Statistical significance was accepted if $P < 0.05$.

RESULTS

Maternal phenotype

Dams fed a high-fat diet consumed approximately 30% less (by weight) than chow-fed dams (C, 29.7 ± 1.0 g/week, $n = 17$; HF, 21.5 ± 1.2 g/week, $n = 21$, $P = 0.003$). The average energy consumption (in kcal) over the 4 weeks immediately before mating did not differ significantly between groups ($P = 0.148$). Dams consuming a high-fat diet before and during pregnancy and suckling were 40% heavier (C, 27.9 ± 0.7 g $n = 17$; HF, 38.7 ± 1.5 g $n = 21$) and had a significantly higher volume and proportion of body fat than those consuming a chow diet (Fig. 2). The lean : fat soft tissue ratio for the C and HF-fed dams was 2.3 ± 0.3 ($n = 5$) and 1.0 ± 0.1 ($n = 6$), respectively ($P = 0.0014$).
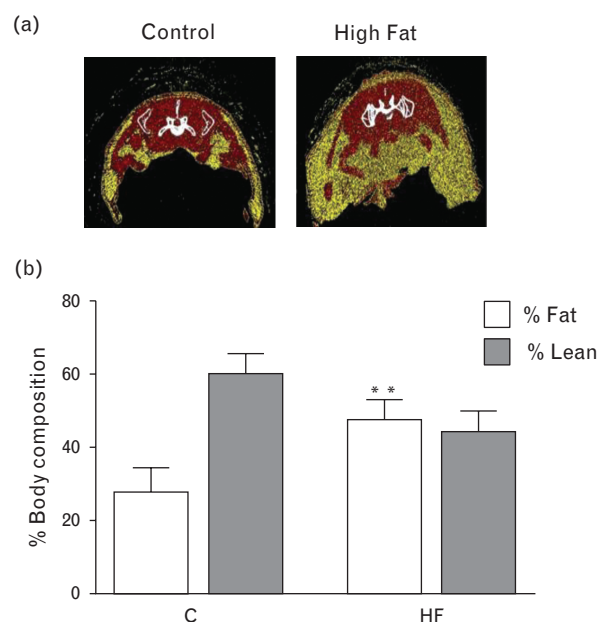

FIGURE 2 Phenotype of dams. (a) Cross-sectional computed tomographic images taken at the top of the pelvis showing fat distribution (shown in yellow) in dams. (b) Percentage body fat and lean-tissue volume estimated by computed tomography imaging (C, $n = 5$; HF, $n = 6$). Data are mean $\pm$ SEM; $**P < 0.0001$ control vs. high-fat dams.

HF-fed dams also exhibited significant hyperglycaemia (C, 7.6 ± 1.2 mmol/l; HF, 10.9 ± 1.3 mmol/l, $n = 6$ per group, $P = 0.03$) as has been shown previously [28,30]. Dam total fasting plasma lipids did not differ between groups (C, 2541 ± 125 μg/ml, HF 2662 ± 257 μg/ml, $n = 6$ per group). HF-fed dams gave birth to smaller litters (C $= 8 \pm 1$, HF 5 ± 1, $P = 0.007$) but there was no significant difference in litter sex balance between the two groups.

Offspring phenotype

The amount of diet consumed (g/week) measured in a subset of offspring over 12 weeks postweaning was significantly lower in offspring fed a fat-rich diet after weaning (C/HF and HF/HF) than that of offspring fed a chow diet after weaning (C/C and HF/C; $P < 0.001$); a finding that is consistent with results from other studies that show mice are capable of caloric regulation is consistent [17]. There was a significant impact of postnatal diet on caloric intake ($F = 5.43$, $P = 0.029$). Caloric intake, however, of offspring consuming a postweaning fat-rich diet (C/HF, 18.9 ± 0.5; HF/HF 21.2 ± 0.9 kcal/week) did not differ significantly from that of C/C (26.7 ± 0.7 kcal/week) or HF/C (27.7 ± 1.0 kcal/week) offspring ($P = 0.06$).

Offspring bodyweight measured in the four dietary groups at 15 weeks of age are shown in Fig. 3a. Body weight was significantly higher in offspring groups exposed to postweaning HF (C/HF and HF/HF; $P < 0.0001$) (prenatal diet, $F = 4.9$, $P = 0.03$; postnatal diet, $F = 74.6$, $P < 0.0001$). Additionally, C/HF and HF/HF offspring had a higher volume and proportion of body fat than C/C or HF/C offspring ($P < 0.0001$) (Fig. 3b and c). The lean : fat tissue ratios for the four groups were C/C, 1.8 ± 0.1; HF/C, 2.8 ± 0.4; C/HF, 1.2 ± 0.4; HF/HF, 0.8 ± 0.1.

Offspring SBP was significantly influenced by both prenatal ($F = 13.6$, $P = 0.001$) and postnatal ($F = 13.2$, $P = 0.002$) diet. Postnatal diet had a greater influence on DBP ($F = 5.6$, $P = 0.001$) than prenatal diet ($F = 3.5$, $P = 0.071$) (Fig. 3d). A postweaning fat-rich diet had a significant impact on fasting plasma glucose levels ($F = 8.5$, $P = 0.009$), with C/HF and HF/HF offspring showing significant hyperglycaemia compared with C/C and HF/C offspring at 15 weeks of age ($P < 0.05$) (Fig. 3e). Offspring total plasma lipids did not differ significantly between dietary groups (μg/ml) (C/C 2619 ± 223, HF/C 3643 ± 370.4, C/HF 3417 ± 520, HF/HF 3486 ± 531, $n = 4$–6 per group).

Impact of maternal high-fat feeding on the contributions of nitric oxide and endothelium-derived hyperpolarization pathways to acetylcholine-induced relaxation in third-order cremaster arterioles

Functional studies were conducted in a total of 41 offspring from the four dietary groups. Data are reported from 33 vessels that exhibited an initial constrictor response to 1 μmol/l noradrenaline of more than 50% of resting diameter and that remained functional throughout the whole protocol. There was no significant difference in the resting diameter of the vessels studied between the

four groups ($P = 0.143$) (Table 1). Initial constrictor response to noradrenaline did not differ across the four dietary groups. The tone generated in response to 1 μmol/l noradrenaline (ratio of noradrenaline-constricted to resting diameter) was for C/C, 0.46 ± 0.05; HF/C 0.40 ± 0.03; C/HF 0.33 ± 0.04; HF/HF 0.51 ± 0.03 ($P = 0.09$). The relaxation response to ACh did not differ significantly between groups (Fig. 4) ($F = 3.96$, $P = 0.057$). The sequential addition of the pharmacological inhibitors L-NAME + indomethacin followed by TRAM-34 + apamin resulted in group-specific reductions in ACh-induced relaxation (Fig. 4a), indicative of differing contributions of the EDRF and EDH signalling pathways to the relaxation of cremaster arterioles across the offspring dietary groups ($F = 5.44$, $P = 0.028$). In C/C arterioles the % contributions of EDH and EDRF to the ACh-induced L-NAME + indomethacin + TRAM-34 + apamin-blockable relaxation were 60 and 40%, respectively. This ratio was similar to that reported previously in isolated myogenically active cremaster arterioles from chow-fed C57BL6 mice [39]. In maternal HF-conditioned (HF/C) offspring EDH contributed less than 10% to ACh-mediated relaxation (EDH : EDRF $= 8 : 92$%) ($P < 0.01$ vs. other dietary groups). EDH : EDRF in C/HF offspring was $51 : 49$% and in offspring exposed to a high-fat diet both before and after weaning (HF/HF) $55 : 45$% (Fig. 4f).

Effect of maternal high-fat feeding on the eNOS mRNA expression in cremaster arterioles

There was a significant effect of diet on expression of eNOS mRNA (prenatal diet $F = 14.8$, $P < 0.001$; postnatal diet $F = 4.9$, $P = 0.058$; interaction prenatal diet∗postnatal diet, $F = 33.1$, $P < 0.001$). The fold change relative to C/C (1.0 ± 0.05) was HF/C 1.2 ± 0.1; C/HF 1.35 ± 0.05; and HF/HF 0.4 ± 0.1 ($P < 0.01$ HF/HF vs. HF/C and C/HF) ($n = 3$ per offspring group).

Effect of maternal high-fat feeding on the expression and localization of intermediate-conductance calcium-activated potassium channel in cremaster arterioles

Figure 5a shows examples of confocal images of maximum projection images from z-stacks of the whole vessel in cremaster arterioles from the four offspring groups. IK_{Ca} expression in cremaster arterioles was influenced by both maternal ($F = 7.7$ $P = 0.017$) and offspring diet ($F = 6.3$, $P = 0.027$) with total expression of IK_{Ca} in HF/HF arterioles greater than that in both HF/C and C/HF arterioles ($P < 0.01$) (Fig. 5c). There was a clear association of IK_{Ca} with the endothelial cell membrane in cremaster arterioles from C/C, C/HF, and HF/HF offspring while staining in those from HF/C offspring appeared diffuse with little overlap with CD31-stained endothelial cell plasma membrane in single transverse median optical section of each vessel (Fig. 5b). Overlap of IK_{Ca} with CD31 was more influenced by postnatal ($F = 9.84$, $P = 0.016$) than prenatal ($F = 0.87$, $P = 0.39$) diet. We were unable to quantify expression and localization of SK_{Ca} in our whole cremaster preparation because of poor antibody staining.
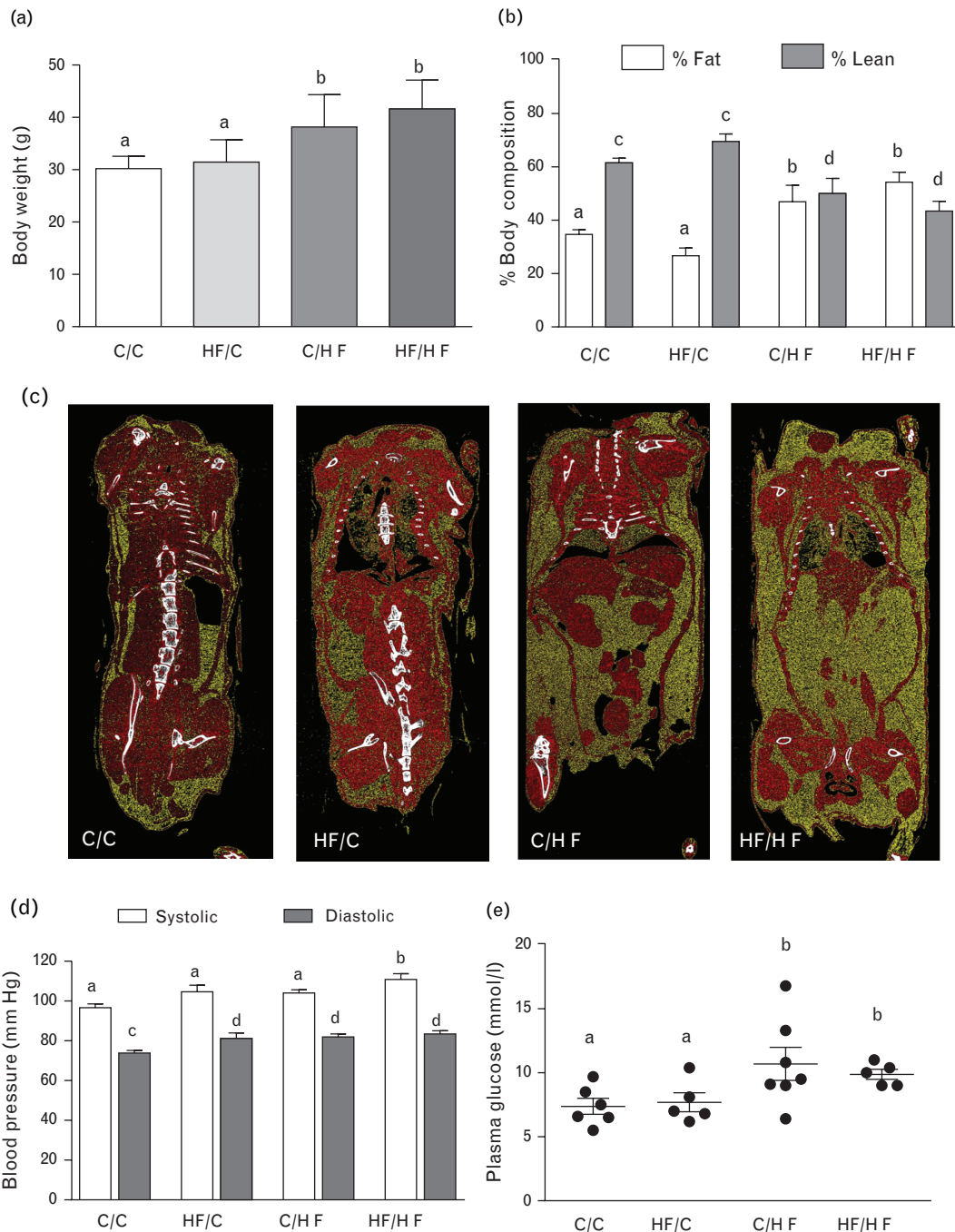
FIGURE 3 Phenotype of male mouse offspring at 15 weeks of age. Dams were fed either a high-fat diet (HF) or standard chow (C) for 4–6 weeks before conception and during gestation and lactation. At weaning, offspring were assigned to a C or HF diet to give four dietary groups C/C, HF/C, C/HF, and HF/HF. Bar graphs represent mean ± SEM. (a) Offspring body weight (C/C, $n = 23$; HF/C, $n = 20$; C/HF, $n = 20$; HF/HF, $n = 18$). (b) Percentage body fat and soft tissue volume from a subset of offspring estimated by computed tomography imaging ($n = 5$/group except C/HF $n = 4$). (c) Longitudinal mid-thoracic sectional computed tomography images showing fat distribution (shown in yellow). (d) SBPs and DBPs measured in a subset of offspring (C/C, $n = 10$; HF/C, $n = 10$; C/HF, $n = 10$; HF/HF, $n = 9$). (e) Fasting plasma glucose from a subset of offspring (mean ± 95% confidence interval) (C/C, $n = 6$; HF/C, C/HF, $n = 5$; $n = 7$; HF/HF, $n = 5$). Values of a given variable that are significantly different ($P < 0.05$) between offspring dietary groups are indicated by different letters.

Impact of maternal high-fat diet on the expression and localization of intermediate-conductance calcium-activated potassium channel in third-order mesenteric arteries

The whole mount cremaster preparation precluded optimal resolution of the endothelial expression and localization of IK_{Ca} because of its complex structure. We therefore went on to further examine the impact of pre and postnatal diet on membrane localization and intracellular expression and of IK_{Ca} in the endothelium of open segments of third-order mesenteric arteries from the same conditioned animals in which it was possible to image the luminal endothelium more clearly. Figure 6 shows maximum projection images

TABLE 1. Diameters of perfused cremaster arterioles before (resting) and during constriction with noradrenaline (noradrenaline, 1 μmol/l) and following application of acetylcholine (10 μmol/l). L-NAME (100 μmol/l) along with indomethacin (10 μmol/l), and TRAM-34 (1 μmol/l) along with apamin (0.1 μmol/l)

Vessel diameter (μm) (mean ± SEM)							
Offspring group	Resting	Noradrenaline	Noradrenaline + ACh	Noradrenaline + L-NAME + INDO	Noradrenaline + L-NAME + INDO + ACh	Noradrenaline + L-NAME + INDO + APA + TRAM-34	Noradrenaline + L-NAME + INDO + APA + TRAM + ACh
C/C (n=8)	26.4±2.3	12.4±1.9	20.3±2.0	9.3±1.1	13.3±1.9	8.3±1.4	9.1±1.5
HF/C (n=7)	20.7±2.3	9.3±1.7	14.3±1.5	7.9±1.4	8.6±1.7	7.0±1.8	7.0±1.8
C/HF (n=11)	20.4±1.2	6.5±0.8	11.5±1.2	5.5±0.4	8.1±0.8	5.2±0.5	5.5±0.6
HF/HF (n=7)	22.1±2.8	12.0±1.6	16.9±2.5	11.0±2.6	14.8±3.6	11.9±1.8	11.1±2.2

ACh, acetylcholine; APA, apamin; INDO, indomethacin; L-NAME, N^{ω}-nitro-L-arginine methyl ester hydrochloride; TRAM-34, 1-[(2-chlorophenyl) diphenylmethyl]-1H-pyrazole.
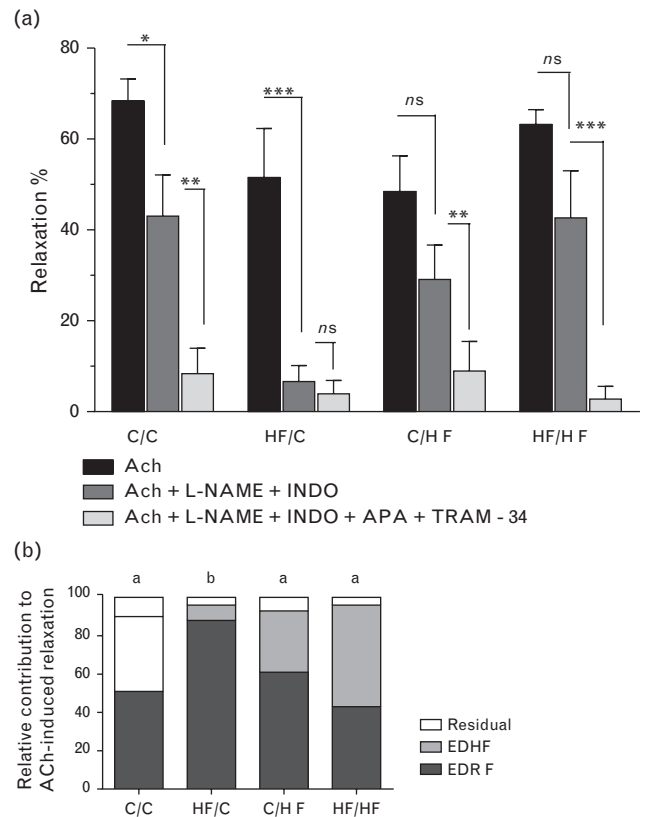

FIGURE 4 Relaxation to ACh in the absence and presence of pharmacological inhibitors in third-order cremaster arterioles of male mice offspring at 15 weeks of age. Dams were fed either a high-fat (HF) diet or standard chow (C) for 4–6 weeks before conception and during gestation and lactation. At weaning, offspring were assigned to a C or HF diet to give four dietary groups C/C, HF/C, C/HF, and HF/HF. (a) ACh-induced relaxations in the absence (black bars) and presence of 100 μmol/l L-NAME + 10 μmol/l INDO (dark grey bars), 100 μmol/l L-NAME + 10 μmol/l INDO + 0.1 μmol/l APA + 1 μmol/l TRAM-34 (light grey bars). Arterioles were preconstricted with 1 μmol/l noradrenaline and change in diameter normalized to the preconstricted diameter. Data are mean ± SEM (C/C $n=8$, HF/C $n=7$, C/HF $n=11$, HF/HF $n=7$). Between treatments in any offspring group: ∗$P < 0.05$, ∗∗$P < 0.01$, ∗∗∗$P < 0.0001$. (b) Relative contribution of endothelium-derived relaxing factors (blockable by L-NAME + INDO), endothelium-derived hyperpolarizing factors (blockable by APA + TRAM-34) and 'Residual' to the ACh-induced relaxation expressed as a proportion of the ACh-relaxation response shown in Fig. 4a. Significant differences ($P < 0.05$) in the relative contributions of endothelium-derived hyperpolariziation to relaxation between offspring groups are indicated by different letters. ACh, acetylcholine; APA, apamin; INDO, indomethacin; L-NAME, N^{ω}-nitro-L-arginine methyl ester hydrochloride; TRAM-34, 1-[(2-chlorophenyl) diphenylmethyl]-1H-pyrazole.

from z-stacks of the endothelial and smooth muscle cell layers of mesenteric arteries viewed from the luminal surface. As in cremaster arterioles, total IK_{Ca} expression in mesenteric arteries was influenced by both maternal ($F=12.1$, $P=0.003$) and offspring diet ($F=6.0$, $P=0.027$; interaction prenatal × postnatal diet, $F=16.77$, $P=0.001$), with total intensity of IK_{Ca} in mesenteric arteries from HF/HF offspring greater than that in both HF/C and C/HF offspring ($P<0.01$) (Fig. 6b). Overlap of IK_{Ca} with the DAPI-stained nuclei of endothelial cells appeared to be influenced by prenatal diet ($F=5.00$, $P=0.04$) with an increase in IK_{Ca}/DAPI overlap in the endothelial layer of the mesenteric arteries from HF/C conditioned offspring ($P=0.004$) (Fig. 6c). By contrast, overlap of IK_{Ca} with CD31 was influenced by postnatal ($F=5.34$, $P=0.03$) but not prenatal ($F=1.2$, $P=0.29$) diet (C/C $6.0±1.7$; HF/C
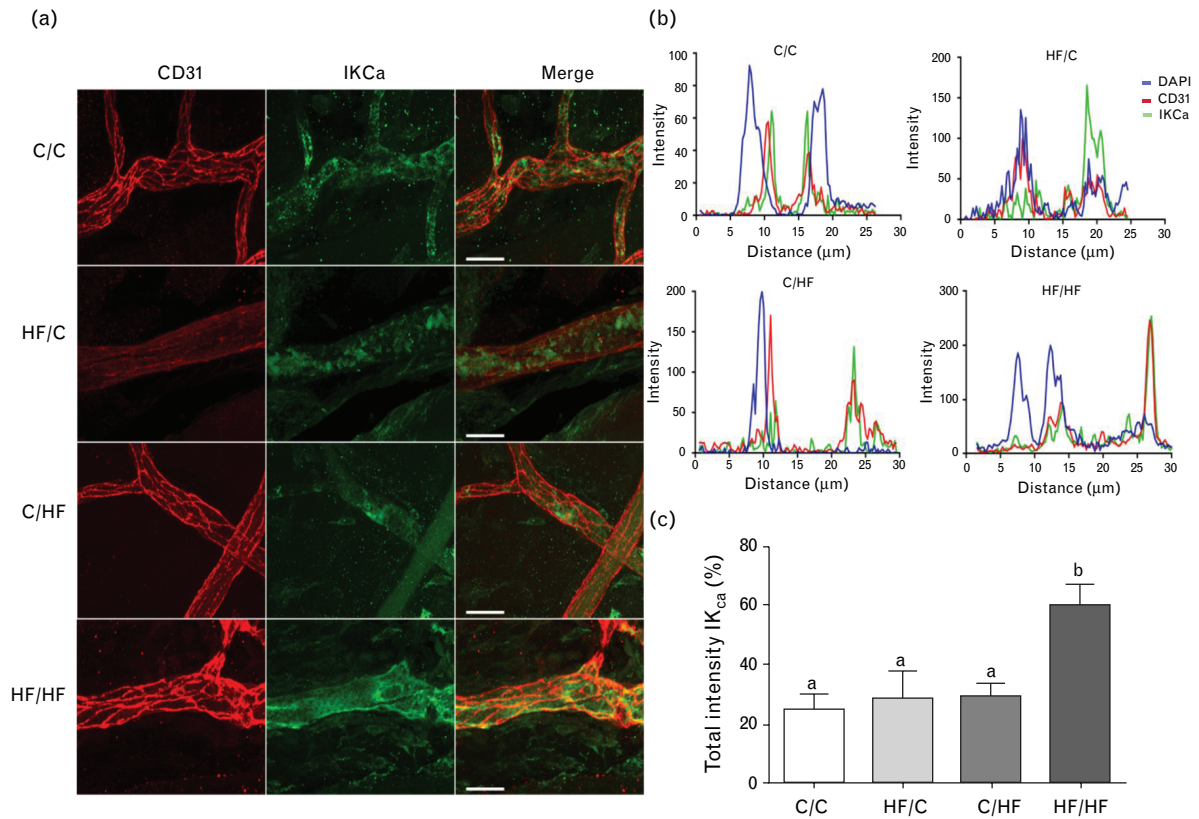
FIGURE 5 Endothelial cell immunohistochemical expression pattern of IK_{Ca} channels in mouse cremaster arterioles from four offspring dietary groups. (a) Confocal images the wall of in-situ arterioles showing expression of CD31 and IK_{Ca}. (b) 4,6-diamidino-2-phenylindole (nucleus)/IK_{Ca}/CD31 colocalization expressed as intensity in a single z plane taken across the diameter of the vessel. (c) Total expression of IK_{Ca} as measured by intensity of IK_{Ca}. Data are mean ± SEM in $n = 3-5$ animals/offspring group. Significant differences ($P < 0.05$) between offspring groups are indicated by different letters. Scale bar = 25 μm. IK_{Ca}, intermediate-conductance calcium-activated potassium channel.
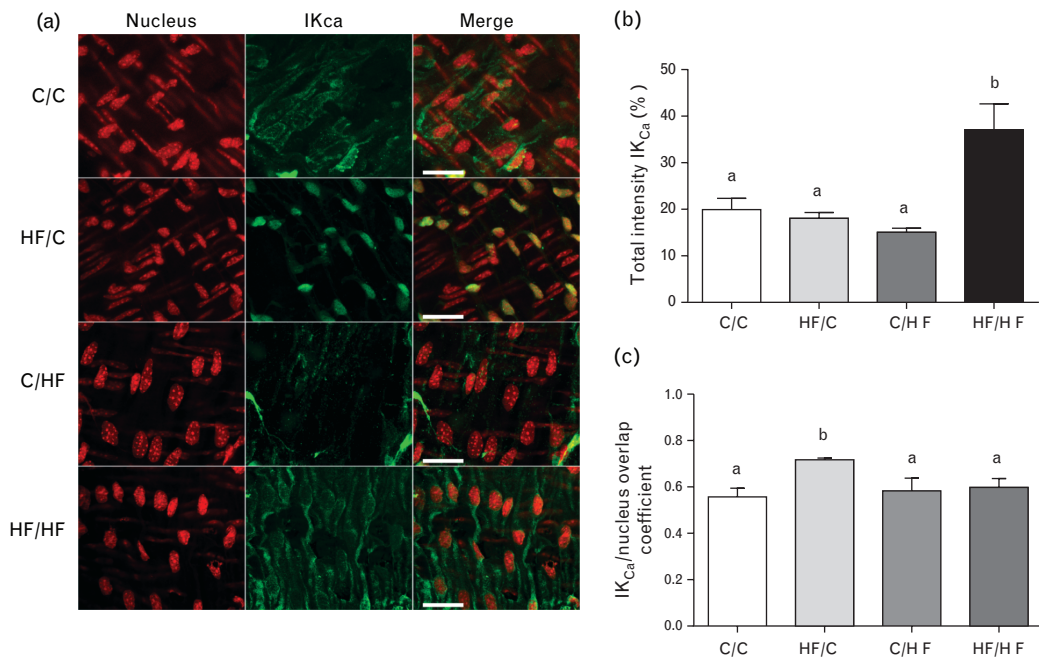
FIGURE 6 Expression and localization of IK_{Ca} in third-order mesenteric arteries from four offspring dietary groups. (a) Confocal images of opened segments of artery showing distribution of nuclei using 4,6-diamidino-2-phenylindole and IK_{Ca} labelling. (b) Intensity of IK_{Ca} calculated from three regions of interest in each vessel (1600 μm²). (c) IK_{Ca} localization with nuclear region of endothelial cells calculated using the Mander's overlap coefficient. Data are mean ± SEM, $n = 4-5$ animals/dietary group. Significant differences ($P < 0.05$) between offspring groups are indicated by different letters. Scale bar = 20 μm. IK_{Ca}, intermediate-conductance calcium-activated potassium channel.

TABLE 2. Distribution of holes in the IEL and colocalization with intermediate-conductance calcium-activated potassium channel in third-order mesenteric arteries from adult male mouse offspring from four dietary groups

	C/C	HF/C	C/HF	HF/HF
Hole density (per $10^3 \, \mu m^2$)	13.6 ± 1.1	15.0 ± 1.9	15.1 ± 2.4	17.1 ± 1.6
Hole diameter (μm)	1.15 ± 0.08	1.33 ± 0.11	1.24 ± 0.08	1.19 ± 0.08
Colocalization with IK_{Ca} (%)	26 ± 3	20 ± 3	27 ± 7	35 ± 4

Number of holes in the IEL expressed per $1000 \, \mu m^2$ IEL area ($n = 10–13$ animals/dietary group. IK_{Ca} localization to IEL holes expressed as a percentage of total holes counted ($n = 4–6$ animals/group). Data are mean ± SEM. There were no significant differences between HF-fed and C/C groups. IEL, internal elastic lamina.

6.7 ± 1.4; C/HF 9.0 ± 1.9; HF/HF 12.5 ± 2.7 ($n = 4–6$ vessels per group).

We also quantified endothelial domains (number and size of holes in the internal elastic lamina and colocalization of IK_{Ca} and SK_{Ca} in the same mesenteric segments. There was no significant difference in the number of IEL holes per unit area or their size in mesenteric arteries from the three HF-fed offspring (HF/C, C/HF and HF/HF) compared with C/C. Neither did the number of holes colocalized with IK_{Ca} differ between groups (Table 2).

DISCUSSION

We have shown that developmental conditioning through exposure to a fat-rich diet *in utero* and during suckling gives rise to distinct alterations in the contribution of EDRF and EDH signalling to ACh-mediated relaxation in skeletal muscle arterioles. Our findings provide evidence that attenuation of functional EDH-mediated relaxation in developmentally conditioned adult male mouse offspring is associated with altered endothelial cell membrane localization and/or trafficking of IK_{Ca} channels. Developmentally conditioned male offspring exposed to a 'second hit' and studied at 15 weeks of age exhibit the ability to upregulate EDH-mediated vasodilatation in the face of a reducing nitric oxide-mediated vasodilator response. Sustained function is accompanied by an increased endothelial expression and/or redistribution of IK_{Ca} channels to preserve EDH-mediated vasodilatation within the skeletal muscle vasculature. These findings evidence a flexibility of the developmentally conditioned EDH-signalling pathway similar to that reported in the early stages of cardiovascular and metabolic disease.

Developmental conditioning of functional relaxation in the microcirculation

The conditioned cardiovascular and metabolic phenotype that we report in 15-week-old male mice offspring of dams fed a diet rich in animal fat for 4–6 weeks before mating and during pregnancy and suckling is similar to that we have reported previously [28] and consistent with that in a wide range of animal models of maternal overnutrition (for review see [35]). It is also similar to that observed in prospective human cohort studies [36] in which associations between maternal nutritional intake and weight gain during pregnancy and offspring growth and metabolic and cardiovascular traits have been demonstrated (for review see [20]). However, the association between the developmental environment, vascular structure and function, and the development of cardiovascular and metabolic disease in adulthood remains contentious and the mechanistic pathways underinvestigated.

Our new findings using perfused skeletal muscle arterioles *in situ* establish that the microvasculature is susceptible to conditioning by the developmental environment, and that this leads to alterations in signal transduction underlying endothelium-dependent dilator responses. The modest (~20%) loss of dilator capacity in skeletal muscle arterioles (<30 μm diameter) in all HF-fed offspring groups was similar to that reported in rat mesenteric resistance arteries [18] and foetal sheep coronary arteries [37] in developmentally conditioned offspring. A similar small but significant reduction has been reported in cremaster muscle arterioles from adult hamster offspring overnourished in early postnatal life by restriction of litter size [38]. If the cremaster skeletal muscle vasculature is taken as a surrogate for that of less accessible skeletal muscle beds [39], it is probable that a similar loss of dilator tone across other organ systems will contribute to an increase in peripheral resistance and the raised BP seen in the conditioned offspring.

In the current study in cremaster arterioles (18–32 μm diameter) where EDH-mediated relaxation might be expected to predominate, the relative contribution of EDH to endothelium-dependent relaxation (via a pathway blocked by apamin and TRAM-34) was reduced from ~60% in chow-fed controls (C/C) to less than 10% in conditioned (HF/C) offspring. Previous studies in dietary conditioned rodent offspring failed to show attenuation of ACh-mediated relaxation in the presence of cyclooxygenase and nitric oxide synthase (NOS) blockade, in large conduit (femoral) arteries in which EDH-mediated vasodilatation has a less prominent role than nitric oxide [11,19]. However, a reduction in EDH-mediated relaxation has been reported in third-order mesenteric resistance arteries from rat offspring of fat-fed dams [11] and in foetal coronary arteries from sheep subject to maternal nutrient restriction during pregnancy [18]. Together these data are consistent with a susceptibility of EDH-signalling to developmental conditioning.

We have previously shown that a second insult (a postweaning fat-rich diet) independently influences vascular outcomes and interacts with the effects of an adverse uterine environment to exacerbate vascular dysfunction [19]. In larger conduit arteries this was in part attributable to an increase in oxidative stress and reduced nitric oxide bioavailability [19]. While there was a significant effect of diet on expression of eNOS mRNA in the cremaster, we saw no significant difference in nitric oxide-mediated relaxation in cremaster arterioles in offspring exposed to a fat-rich diet both pre and postweaning (HF/HF) compared with C/HF or

HF/C offspring. To what extent this is attributable to altered reduction-oxidation balance has yet to be elucidated. The contribution of EDH to ACh-induced relaxation of HF/HF offspring was more than four times greater than that seen in arterioles from HF/C offspring and similar to that seen in the other offspring groups. These data suggest an adaptive mechanism to preserve dilator function and ameliorate any reduction in other signalling pathways. This adaptive response appears similar to that seen in the diet-induced obese rat saphenous artery [8] and in coronary arteries of the Zucker rat in the early stages of obesity [9] in which enhanced EDH-mediated relaxation appears to compensate for the loss of nitric oxide-mediated relaxation. A similar plasticity has been reported in foetal and neonatal whereby there is a maturational switch in the signalling pathways controlling vasodilatation from one dominated by EDH to one in which nitric oxide plays a more prominent role [5,24,32,36,38]. The prominent role of EDH-mediated relaxation during early life may also render this signalling pathway susceptible to developmental conditioning. Whether the susceptibility of the EDH pathway to developmental conditioning that we observe in the HF/C adult offspring is a consequence of the dominance of EDHs in endothelium-dependent relaxation during vascular development and maturation, and whether a conditioned imbalance in EDH:EDRF is a risk factor for adult vascular disease, requires further investigation.

We did not observe a significant alteration in EDH:EDRF in C/HF mouse offspring compared with control. The reasons for this are unclear. Similar to the HF/HF offspring, C/HF offspring were heavier, with more body fat, higher BP and a trend to dysglycaemia compared with chow-fed control offspring. It is possible that had we continued the offspring on a fat-rich diet for longer and studied the animals at an older age they would have gone on to show an even greater attenuation of dilator responses similar to those reported previously in larger blood vessels from 30-week-old fat-fed mouse offspring [19].

Developmental conditioning of intermediate-conductance calcium-activated potassium channel signalling in the microcirculation

In the present study, we have shown that expression and cellular localization of IK_{Ca} channels in the endothelium of both cremaster arterioles and third-order mesenteric resistance arteries was influenced by both maternal and postnatal offspring diet. The physiological response of ion channels depends critically on their number and time spent at the cell surface [27]. Nuclear localization of IK_{Ca} has been demonstrated in bronchial smooth muscle cells in healthy and asthmatic airways [40] and in the human placental syncytiotrophoblast from normal term placentas [41] where it may be associated with cell proliferation and differentiation. Moreover, studies in an eccrine sweat gland cell line have shown agonist-induced intracellular trafficking of IK_{Ca} to and from the nuclear region [42]. Thus, it is possible that the reduced endothelial plasma membrane association and increased intracellular accumulation of IK_{Ca} in developmentally conditioned (HF/C) animals may be indicative of an altered anterograde/retrograde trafficking of IK_{Ca} resulting in attenuation of EDH-mediated relaxation.

Attenuation in functional EDH signalling in HF/C cremaster arterioles was not, as anticipated, associated with either a decrease in total IK_{Ca} expression or changes in the localization of channels to regions adjacent to the myoendothelial domain; as seen in obesity [8]. However, an increased nuclear association of IK_{Ca} was seen in the endothelium of mesenteric arteries taken from the same animals. Thus it is possible that IK_{Ca} trafficking may partially explain the reduced EDH-mediated relaxation reported in third-order mesenteric resistance arteries from rat offspring of fat-fed dams [11].

A marked increase in endothelial (CD31-associated) expression of IK_{Ca} was seen in the vascular endothelium from HF/HF offspring. The increase in IK_{Ca} expression in HF/HF offspring was consistent with the observed reversal in relative contribution of EDH:EDRF to ACh-mediated relaxation from one dominated by EDRF-type (nitric oxide) relaxation in HF/C offspring to one in which EDH predominated. Our observations are supported by those of Climent et al. [9] who showed increased function and expression of IK_{Ca} and SK_{Ca} to preserve dilator function in animals exhibiting early stages of the metabolic syndrome, hypertension, and obesity.

We observed little change in endothelial expression of IK_{Ca} in C/HF offspring compared with C/C. IK_{Ca} signalling is altered with advancing age [24] and age interacts with maternal and offspring diet to worsen the vascular phenotype [28]. It is possible that we would have detected more marked changes in expression and localization of K_{Ca} channels had we studied older C/HF offspring with a more advanced cardio-metabolic phenotype.

The mechanisms underlying altered expression and activity of IK_{Ca} channels at the endothelial cell surface remain unclear. Protein glycosylation may play a key role in this process [43] and advanced glycation end products and oxidative stress – as exhibited by fat-rich diet conditioned offspring [28] have been shown to impair both expression and activity of K_{Ca} channels [44,45]. Similarly, endoplasmic reticular stress has been shown to impair IK_{Ca} channel-mediated relaxation in porcine coronary arteries and to inhibit the endothelial cell surface expression of IK_{Ca} channels [46]. To what extent this represented reduced forward trafficking or enhanced endocytosis of channels remained unclear.

Study limitations

We studied the independent effects of a preweaning fat-rich diet and the subsequent impact of a postweaning high-fat diet on the conditioned phenotype on skeletal muscle arterioles in male mouse offspring at 15 weeks of age using a perfused cremaster preparation. The relative contribution of EDH to ACh-mediated relaxation in perfused cremaster arterioles was not as great as anticipated considering the size and location of the vessels studied. This may be because of the use of a perfused preparation and the lack of endogenous vascular tone which necessitates preconstruction of the vessels with noradrenaline. However, although an agonist was used to generate tone, the

percentage decrease in diameter was matched to that observed in in-vivo cremaster preparation [47,19].

The use of the cremaster muscle preparation precluded the study of female offspring. Sex differences in the relative contributions of nitric oxide and EDH to agonist-induced endothelium-dependent relaxation have been reported in resistance arteries [48] and EDH to dominate in arteries of females [49]. Further, oestrogens have been shown to target IK_{Ca} channels and to induce translocation and activation [42]. Sexual dimorphism has also been demonstrated in the vascular response of conditioned offspring [50]. Our findings in male offspring should therefore be extrapolated across the sexes with caution.

In conclusion, we provide the first evidence that developmental conditioning through exposure to fat-rich diet during gestation and suckling gives rise to changes in the relative contribution of the EDH-signalling pathway to vasorelaxation in skeletal muscle microvasculature. Conditioned attenuation in functional EDH-mediated relaxation is associated with a reduction in endothelial expression and trafficking of IK_{Ca} channels. However, our findings suggest that conditioning of EDH-signalling does not appear to disadvantage adult offspring, nor negate the protection afforded by the EDH pathway, in the short term. Continuing exposure to an adverse environment in adult life (post-weaning HF) may induce activation of adaptive vascular mechanisms to preserve the dilator capacity in the face of reduced nitric oxide bioavailability. The match in prenatal and postnatal diet in the HF/HF offspring may serve to advantage these individuals compared with the mismatch in the C/HF and HF/C groups [51]. The capacity for adjustment in EDH-signalling pathways may provide a critical window(s) during which changes in vascular tone associated with cardiovascular disease could be therapeutically targeted.

ACKNOWLEDGEMENTS

The study was conceived and designed by G.F.C., P.A.F. and C.T. M.G.M., R.R., C.T. and R.L.S. carried out all tasks related to the experimental model. Functional experiments were conducted by M.G.M. R.L.S. performed the molecular experiments. M.G.M., C.L.B., R.L.S., R.R. and D.A.J. undertook the confocal imaging studies. S.A.L. performed and analyzed the computed tomography imaging study. Data analysis and interpretation were carried out by R.L.S., M.G.M., C.L.B., C.T., P.A.F. and G.F.C. The manuscript was written by R.L.S. and G.F.C. with input from M.G.M., C.T. and P.A.F. All authors reviewed and approved the final version of the study.

This work has been presented in part to the Physiological Society Annual meeting 2014.

Conflicts of interest

There are no conflicts of interest.

REFERENCES

1. Costa RR, Villela NR, Souza M, Boa BC, Cyrino FZ, Silva SV, *et al.* High fat diet induces central obesity, insulin resistance and microvascular dysfunction in hamsters. *Microvasc Res* 2011; 82:416–422.
2. Frisbee JC. Reduced nitric oxide bioavailability contributes to skeletal muscle microvessel rarefaction in the metabolic syndrome. *Am J Physiol Regul Integr Comp Physiol* 2005; 289:R307–R316.
3. Lesniewski LA, Zigler ML, Durrant JR, Nowlan MJ, Folian BJ, Donato AJ, *et al.* Aging compounds western diet-associated large artery endothelial dysfunction in mice: prevention by voluntary aerobic exercise. *Exp Gerontol* 2013; 48:1218–1225.
4. Muller-Delp JM. Aging-induced adaptations of microvascular reactivity. *Microcirculation* 2006; 13:301–314.
5. Stapleton PA, Goodwill AG, James ME, Frisbee JC. Altered mechanisms of endothelium-dependent dilation in skeletal muscle arterioles with genetic hypercholesterolemia. *Am J Physiol Regul Integr Comp Physiol* 2007; 293:R1110–R1119.
6. Grgic I, Kaistha BP, Hoyer J, Kohler R. Endothelial Ca+ -activated K+ channels in normal and impaired EDHF-dilator responses: relevance to cardiovascular pathologies and drug discovery. *Br J Pharmacol* 2009; 157:509–526.
7. Zhang LN, Vincelette J, Chen D, Gless RD, Anandan SK, Rubanyi GM, *et al.* Inhibition of soluble epoxide hydrolase attenuates endothelial dysfunction in animal models of diabetes, obesity and hypertension. *Eur J Pharmacol* 2011; 654:68–74.
8. Chadha PS, Haddock RE, Howitt L, Morris MJ, Murphy TV, Grayson TH, *et al.* Obesity up-regulates intermediate conductance calcium-activated potassium channels and myoendothelial gap junctions to maintain endothelial vasodilator function. *J Pharmacol Exp Ther* 2010; 335:284–293.
9. Climent B, Moreno L, Martinez P, Contreras C, Sanchez A, Perez-Vizcaino F, *et al.* Upregulation of SK3 and IK1 channels contributes to the enhanced endothelial calcium signaling and the preserved coronary relaxation in obese Zucker rats. *PLoS One* 2014; 9:e109432.
10. Ashraf MZ, Reddy MK, Hussain ME, Podrez EA, Fahim M. Contribution of EDRF and EDHF to restoration of endothelial function following dietary restrictions in hypercholesterolemic rats. *Indian J Exp Biol* 2007; 45:505–514.
11. Wolfle SE, de WC. Intact endothelium-dependent dilation and conducted responses in resistance vessels of hypercholesterolemic mice in vivo. *J Vasc Res* 2005; 42:475–482.
12. Haddock RE, Grayson TH, Morris MJ, Howitt L, Chadha PS, Sandow SL. Diet-induced obesity impairs endothelium-derived hyperpolarization via altered potassium channel signaling mechanisms. *PLoS One* 2011; 6:e16423.
13. Leo CH, Hart JL, Woodman OL. Impairment of both nitric oxide-mediated and EDHF-type relaxation in small mesenteric arteries from rats with streptozotocin-induced diabetes. *Br J Pharmacol* 2011; 162:365–377.
14. Barker DJ, Osmond C. Infant mortality, childhood nutrition, and ischaemic heart disease in England and Wales. *Lancet* 1986; 1:1077–1081.
15. Gluckman PD, Hanson MA, Cooper C, Thornburg KL. Effect of in utero and early-life conditions on adult health and disease. *N Engl J Med* 2008; 359:61–73.
16. Drake AJ, Reynolds RM. Impact of maternal obesity on offspring obesity and cardiometabolic disease risk. *Reproduction* 2010; 140:387–398.
17. Parekh PI, Petro AE, Tiller JM, Feinglos MN, Surwit RS. Reversal of diet-induced obesity and diabetes in C57BL/6J mice. *Metabolism* 1998; 47:1089–1096.
18. Taylor PD, Khan IY, Hanson MA, Poston L. Impaired EDHF-mediated vasodilatation in adult offspring of rats exposed to a fat-rich diet in pregnancy. *J Physiol* 2004; 558 (Pt 3):943–951.
19. Wolfle SE, Schmidt VJ, Hoyer J, Kohler R, de WC. Prominent role of KCa3.1 in endothelium-derived hyperpolarizing factor-type dilations and conducted responses in the microcirculation in vivo. *Cardiovasc Res* 2009; 82:476–483.
20. Clough GF. Developmental conditioning of the vasculature. *Compr Physiol* 2015; 5:397–438.
21. Dora KA, Sandow SL, Gallagher NT, Takano H, Rummery NM, Hill CE, *et al.* Myoendothelial gap junctions may provide the pathway for EDHF in mouse mesenteric artery. *J Vasc Res* 2003; 40:480–490.

22. Edwards G, Feletou M, Weston AH. Endothelium-derived hyperpolarising factors and associated pathways: a synopsis. *Pflugers Arch* 2010; 459:863–879.

23. Stankevicius E, Lopez-Valverde V, Rivera L, Hughes AD, Mulvany MJ, Simonsen U. Combination of Ca2+ -activated K+ channel blockers inhibits acetylcholine-evoked nitric oxide release in rat superior mesenteric artery. *Br J Pharmacol* 2006; 149:560–572.

24. Behringer EJ, Shaw RL, Westcott EB, Socha MJ, Segal SS. Aging impairs electrical conduction along endothelium of resistance arteries through enhanced Ca2 + -activated K + channel activation. *Arterioscler Thromb Vasc Biol* 2013; 33:1892–1901.

25. Brahler S, Kaistha A, Schmidt VJ, Wolfle SE, Busch C, Kaistha BP, et al. Genetic deficit of SK3 and IK1 channels disrupts the endothelium-derived hyperpolarizing factor vasodilator pathway and causes hypertension. *Circulation* 2009; 119:2323–2332.

26. Sandow SL, Goto K, Rummery NM, Hill CE. Developmental changes in myoendothelial gap junction mediated vasodilator activity in the rat saphenous artery. *J Physiol* 2004; 556 (Pt 3):875–886.

27. Balut CM, Hamilton KL, Devor DC. Trafficking of intermediate (KCa3.1) and small (KCa2.x) conductance, Ca(2+)-activated K(+) channels: a novel target for medicinal chemistry efforts? *ChemMedChem* 2012; 7:1741–1755.

28. Torrens C, Ethirajan P, Bruce KD, Cagampang FR, Siow RC, Hanson MA, et al. Interaction between maternal and offspring diet to impair vascular function and oxidative balance in high fat fed male mice. *PLoS One* 2012; 7:e50671.

29. van HM, Compton DS, France CF, Tedesco RP, Fawzi AB, Graziano MP, et al. Diet-induced obese mice develop peripheral, but not central, resistance to leptin. *J Clin Invest* 1997; 99:385–390.

30. Bruce KD, Cagampang FR, Argenton M, Zhang J, Ethirajan PL, Burdge GC, et al. Maternal high-fat feeding primes steatohepatitis in adult mice offspring, involving mitochondrial dysfunction and altered lipogenesis gene expression. *Hepatology* 2009; 50:1796–1808.

31. Kelsall CJ, Hoile SP, Irvine NA, Masoodi M, Torrens C, Lillycrop KA, et al. Vascular dysfunction induced in offspring by maternal dietary fat involves altered arterial polyunsaturated fatty acid biosynthesis. *PLoS One* 2012; 7:e34492.

32. Lanham SA, Cagampang FR, Oreffo RO. Maternal high-fat diet and offspring expression levels of vitamin K-dependent proteins. *Endocrinology* 2014; 155:4761.

33. Baez S. An open cremaster muscle preparation for the study of blood vessels by in vivo microscopy. *Microvasc Res* 1973; 5:384–394.

34. Manders EMM, Verebeek FJ, Aten JA. Measurement of co-localization of objects in dual-colour confocal images. *J Microsc* 1993; 169:375–382.

35. Ainge H, Thompson C, Ozanne SE, Rooney KB. A systematic review on animal models of maternal high fat feeding and offspring glycaemic control. *Int J Obes (Lond)* 2011; 35:325–335.

36. Fraser A, Tilling K, Macdonald-Wallis C, Sattar N, Brion MJ, Benfield L, et al. Association of maternal weight gain in pregnancy with offspring obesity and metabolic and vascular traits in childhood. *Circulation* 2010; 121:2557–2564.

37. Shukla P, Ghatta S, Dubey N, Lemley CO, Johnson ML, Modgil A, et al. Maternal nutrient restriction during pregnancy impairs an endothelium-derived hyperpolarizing factor-like pathway in sheep fetal coronary arteries. *Am J Physiol Heart Circ Physiol* 2014; 307:H134–H142.

38. Leite RD, Kraemer-Aguiar LG, Boa BC, Cyrino FZ, Nivoit P, Bouskela E. Muscle endothelial-dependent microvascular dysfunction in adulthood due to early postnatal overnutrition. *Microvasc Res* 2012; 84:94–98.

39. Potocnik SJ, McSherry I, Ding H, Murphy TV, Kotecha N, Dora KA, et al. Endothelium-dependent vasodilation in myogenically active mouse skeletal muscle arterioles: role of EDH and K(+) channels. *Microcirculation* 2009; 16:377–390.

40. Diaz P, Wood AM, Sibley CP, Greenwood SL. Intermediate conductance Ca2+ -activated K+ channels modulate human placental trophoblast syncytialization. *PLoS One* 2014; 9:e90961.

41. Chachi L, Shikotra A, Duffy SM, Tliba O, Brightling C, Bradding P, et al. Functional KCa3.1 channels regulate steroid insensitivity in bronchial smooth muscle cells. *J Immunol* 2013; 191:2624–2636.

42. Muchekehu RW, Harvey BJ. Estradiol rapidly induces the translocation and activation of the intermediate conductance calcium activated potassium channel in human eccrine sweat gland cells. *Steroids* 2009; 74:212–217.

43. Mant A, Williams S, Roncoroni L, Lowry E, Johnson D, O'Kelly I. N-glycosylation-dependent control of functional expression of background potassium channels K2P3.1 and K2P9.1. *J Biol Chem* 2013; 288:3251–3264.

44. Su J, Lucchesi PA, Gonzalez-Villalobos RA, Palen DI, Rezk BM, Suzuki Y, et al. Role of advanced glycation end products with oxidative stress in resistance artery dysfunction in type 2 diabetic mice. *Arterioscler Thromb Vasc Biol* 2008; 28:1432–1438.

45. Zhao LM, Wang Y, Ma XZ, Wang NP, Deng XL. Advanced glycation end products impair K(Ca)3.1- and K(Ca)2.3-mediated vasodilatation via oxidative stress in rat mesenteric arteries. *Pflugers Arch* 2014; 466:307–317.

46. Wang XC, Sun WT, Yu CM, Pun SH, Underwood MJ, He GW, et al. ER stress mediates homocysteine-induced endothelial dysfunction: modulation of IKCa and SKCa channels. *Atherosclerosis* 2015; 242:191–198.

47. Hungerford JE, Sessa WC, Segal SS. Vasomotor control in arterioles of the mouse cremaster muscle. *FASEB J* 2000; 14:197–207.

48. McCulloch AI, Randall MD. Sex differences in the relative contributions of nitric oxide and EDHF to agonist-stimulated endothelium-dependent relaxations in the rat isolated mesenteric arterial bed. *Br J Pharmacol* 1998; 123:1700–1706.

49. Chan MV, Bubb KJ, Noyce A, Villar IC, Duchene J, Hobbs AJ, et al. Distinct endothelial pathways underlie sexual dimorphism in vascular auto-regulation. *Br J Pharmacol* 2012; 167:805–817.

50. Morton JS, Rueda-Clausen CF, Davidge ST. Mechanisms of endothelium-dependent vasodilation in male and female, young and aged offspring born growth restricted. *Am J Physiol Regul Integr Comp Physiol* 2010; 298:R930–R938.

51. Bateson P, Gluckman P, Hanson M. The biology of developmental plasticity and the Predictive Adaptive Response hypothesis. *J Physiol* 2014; 592 (Pt 11):2357–2368.

Reviewers' Summary Evaluations

Reviewer 1

Developmental conditioning via a high fat diet (HFD) through gestation and suckling may alter the contribution of endothelium-derived hyperpolarization (EDH) to vasorelaxation. In an elegant set of experiments, this study found that developmental conditioning alters EDH contribution to acetylcholine-induced vasorelaxation in the cremaster circulation. Findings could be extended to determine whether EDH signalling is similarly altered in response to other vasodilators and in other vascular beds. Alternative methods, such as measurement of membrane potential, to account for the alteration of EDH signalling in developmental conditioning is also warranted.

Reviewer 2

This is an interesting study on developmental effects of the interaction between maternal and offspring dietary fat intake on Endothelium-derived hyperpolarizing factor (EDHF) in the arterioles of the mouse cremaster muscle. Interestingly, EDHF seems to function normally when high fat intake in prenatal life is matched by high fat intake in postnatal life. Whether this is also the case in humans, particularly in arterioles at other anatomic locations, remains to be seen.